Excited States of the Photosynthetic Reaction Center of *Rhodopseudomonas viridis*: SAC−CI Study

J. Hasegawa,[†] K. Ohkawa,[†] and H. Nakatsuji*[,†,§]

Department of Synthetic Chemistry and Biological Chemistry, Graduate School of Engineering, Kyoto University, Sakyo-ku, Kyoto 606-8501, Japan, and Institute for Fundamental Chemistry, 34-4 Takano Nishi-hiraki-cho, Sakyo-ku, Kyoto 606-8103, Japan

Received: July 2, 1998; In Final Form: September 16, 1998

The excitation spectrum of the photosynthetic reaction center (PSRC) of *Rhodopseudomonas* (*Rps.*) *viridis* is assigned by using the SAC(symmetry adapted cluster)−CI(configuration interaction) method. All the chromophores included in the PSRC, bacteriochlorophyll *b* dimer (special pair, P), bacteriochlorophyll *b* in L- and M-branches (B_L and B_M), bacteriopheophytin *b* in L- and M-branches (H_L and H_M), menaquinone (MQ), ubiquinone (UQ), and four different hemes, c-552, c-554, c-556, and c-559 in c-type cytochrome subunit, were calculated within the environment of proteins, waters, and the other chromophores which were dealt with by the point-charge electrostatic model. We have assigned successfully all the peaks in the experimental spectrum in the energy range from 1.2 to 2.5 eV. The assignment was done by comparing the SAC−CI theoretical spectrum with the experimental one in excitation energy, oscillator strength, linear dichroism data (angle of transition moment), and other experimental information available. Almost all the peaks were red shifted due to the effect of proteins. The present assignment of the spectrum would give a basis for future photoexperimental studies of the PSRC.

I. Introduction

The initial step of solar energy conversion to chemical energy is performed in the photosynthetic reaction center (PSRC) of green plants and some bacteria.[1] The functions of the PSRC are of global significance and offer quite challenging subjects to be clarified by means of science and technology. For the PSRC of *Rhodopseudomonas viridis* (*Rps. viridis*), the X-ray structure was reported by Deisenhofer et al.[2] Figure 1 shows the three-dimensional arrangement of the chromophores involved. An excitation of special pair (P, bacteriochlorophyll *b* dimer) by a light absorption or by an energy transfer from antenna molecules is the first step of the photosynthesis and causes a primary electron transfer in the PSRC.[1] This electron transfer occurs quite efficiently only through the L-branch up to ubiquinone (UQ),[3,4] and the positive charge of P is reduced by an electron transfer from the cytochrome *c* subunit.

In the upper side of Figure 2, the absorption and linear dichroism (LD) spectra of the PSRC of *Rps. viridis* reported by Breton[5] are shown. The spectra show complex but beautiful structures in the region from about 1050 nm to about 450 nm. The peaks in the absorption spectrum are numbered by I−XIV in order of increasing energy. The LD spectrum gives the information on the angle of the transition moment of the excited state from the principal pseudo-C_2 axis of the PSRC. Breton[5] also reported the absorption and LD spectra for the PSRC with the primary donor chemically oxidized (state P^+), which are also shown in the lower part of Figure 2. Recently, van Grondelle and co-workers reported the results indicating new pathways of the electron transfer starting from the excited state of bacteriochlorophyll of *Rhodobacter sphaeroides* (*Rb. sphaeroides*).[6,7] This implies a possibility of an existence of an entirely different electron-transfer pathway involving different excited states of chromophores. In such studies, a precise knowledge on the nature of the excited states in the excitation spectrum of PSRC is very important. Thus, the assignment of the PSRC spectrum shown in Figure 2 and the knowledge on the natures of the excited states involved would provide us a starting point for future photochemical studies involving the PSRC.

Previously, some semiempirical calculations for the excitation spectrum were reported.[8−10] These works qualitatively reproduced the experimental features of the spectrum and brought important information about the excited states. Nevertheless, it is necessary to perform more reliable theoretical assignment by ab initio method because of a limited accuracy of the semiempirical method they used.

Recently, the ab initio electronic structure theory has achieved chemical accuracy, and applications of such methods to large systems, such as biochemically important systems, constitute a challenging frontier of quantum chemistry. Among such theories, the SAC(symmetry adapted cluster)[11]/SAC−CI(configuration interaction)[12]method is very promising.[12−14] It describes almost all kinds of electronic states of molecules in good accuracy including electron correlations: it is applicable to the ground and excited states of molecules from singlet to septet spin multiplicities. The method has been applied to many different kinds of molecules in many different fields of chemistry, and through such applications, the reliability and the usefulness of the method have been established.[13,14] Recently, the SAC/SAC−CI method has been successfully applied to larger molecules, including porphyrin compounds, such as free base porphin,[15] Mg porphin,[16] iron-porphyrin,[17−19] bacteriochlorin and pheophytin,[20] phthalocyanine,[21] etc., and its potential applicability to the excited states of such moderately large systems has been confirmed.

* To whom correspondence should be addressed.
[†] Kyoto University.
[§] Institute for Fundamental Chemistry.

10.1021/jp982869y CCC: $15.00
Published on Web 11/05/1998

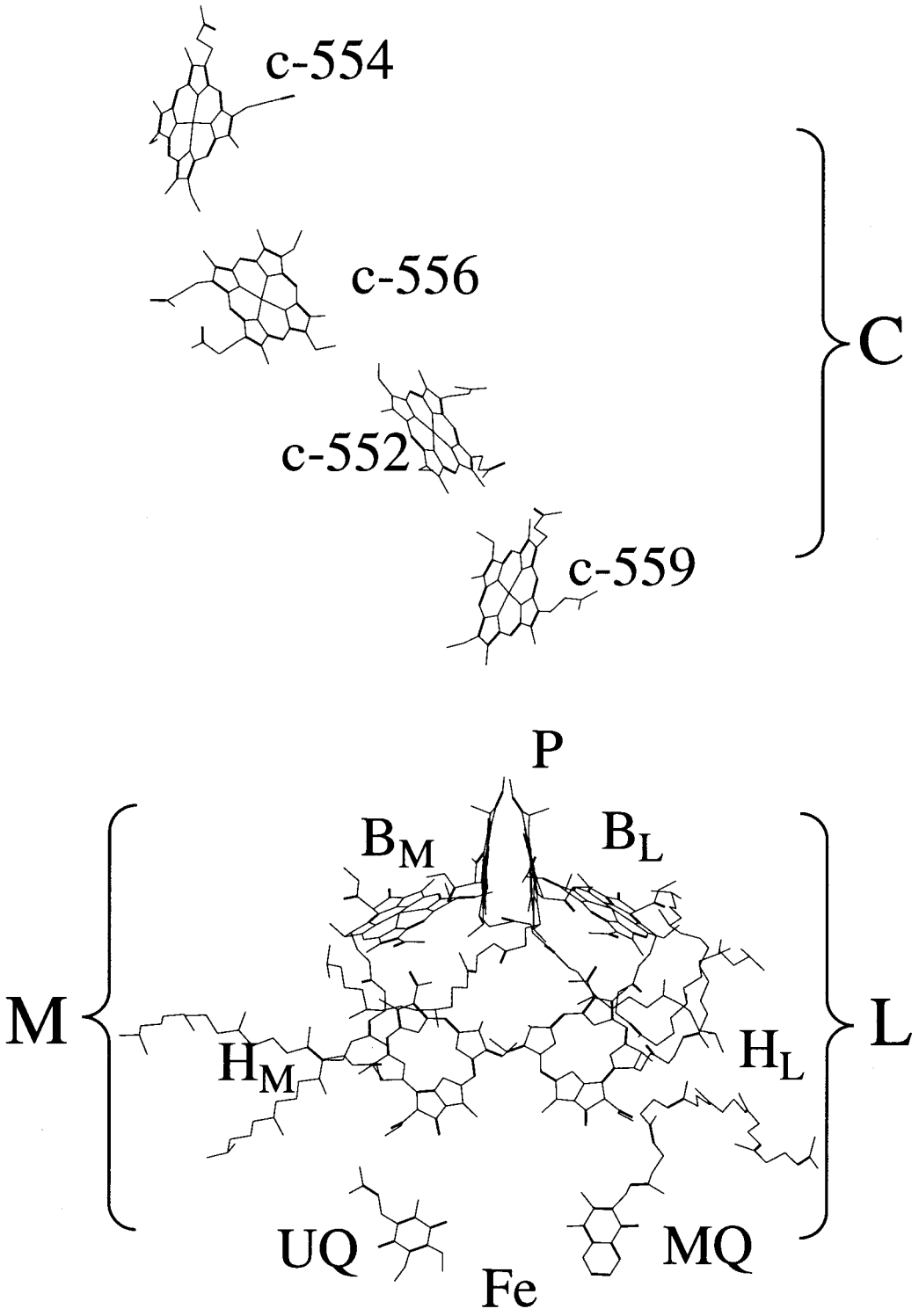

Figure 1. Structure of the chromophores in the PSRC of *Rps. viridis*. The nuclear coordinates are taken from ref 2.

In this paper, we aim to assign the absorption spectrum of the PSRC of *Rps. viridis* shown in Figure 2 by means of the SAC/SAC−CI method and we want to understand the excited electronic structures of the PSRC. We performed calculations for the ground and excited states of all the chromophores involved in the PSRC of *Rps. viridis* in the environment of the proteins and waters, which are approximated by the point-charge electrostatic model. The chromophores for which calculations were performed in this paper are special pair (P) ($Mg_2C_{50}N_8O_4H_{36}$), which is bacteriochlorophyll *b* dimer, bacteriochlorophyll *b* ($MgC_{24}N_4O_2H_{16}$) in L- and M-branches (B_L and B_M), bacteriopheophytin *b* ($C_{24}N_4O_2H_{18}$) in L- and M-branches (H_L and H_M), menaquinone (MQ) ($C_{16}O_2H_{16}$), ubiquinone (UQ) ($C_{14}O_4H_{18}$), and four different hemes, c-552 ($FeC_{26}N_8H_{18}$), c-554, c-556, and c-559 ($FeC_{25}N_6SH_{21}$) in the c-type cytochrome subunit, where the latter three hemes have the same chemical formula but have different geometries and different protein environments. The chromophores in the L- and M-branches are arranged almost symmetrically. We also calculate the excited states of bacteriochlorophyll *b* monomer to understand the spectrum of the dimer, P. A short communication of this study has been published elsewhere.[22]

The calculational details are described in the next section and the excited electronic structures of special pair are investigated

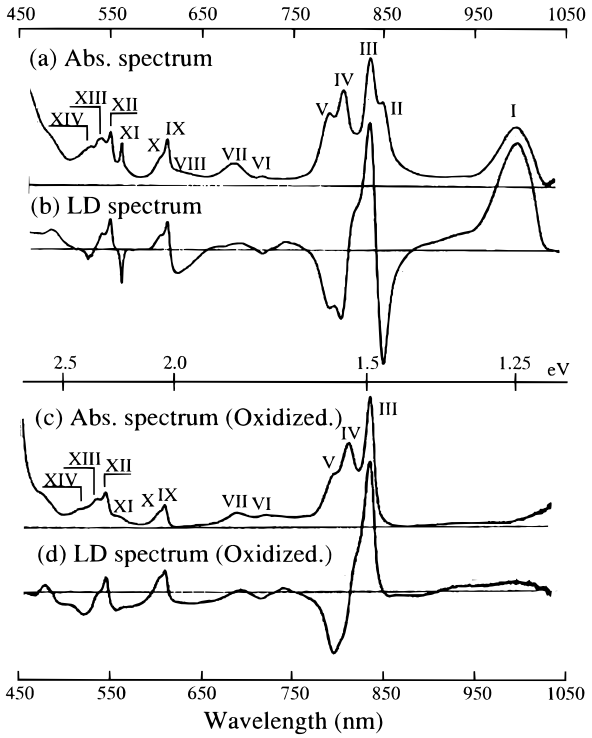

Figure 2. (a) Absorption and (b) linear dichroism (LD) spectra of PSRC of *Rps. viridis*.[5] (c) Absorption and (d) LD spectra of PSRC of *Rps. viridis* with P in its oxidized state (P^+).[5] Intensity is in a relative unit.

in some detail in the subsequent section, comparing with the excited states of the monomer. The detailed discussions on the assignments of the peaks in the experimental excitation spectrum of the PSRC are then given. The assignments are done by utilizing the information on the peak position, intensity, the linear dichroism (LD) data and other available experimental observations. The protein effects are discussed in some detail, and the conclusion of the present study is given in the last section.

II. Computational Details

The structure of the PSRC of *Rps. viridis*[2] is shown in Figure 1. The SAC/SAC−CI calculations are performed for all the chromophores involved in the PSRC. The X-ray crystallographic structure[2] (1PRC in Brookhaven Data Bank[23]) was used for the geometries of the chromophores, and therefore, all the chromophores were treated without symmetry. For calculational efficiency, some substituents in the chromophores were replaced with hydrogens, except for the substituents which can π-conjugate with the rings. The adopted models are shown in Figure 3, where the labeling of the atoms and the rings are indicated. Such simplification was shown to be acceptable in our previous calculations.[20] Though the chemical structures of the three models of the hemes, c554, c556, and c559 are the same, their geometries and the protein environments are different in the X-ray structure.

Common basis sets are taken for all the chromophores. For C, N, and O atoms, Huzinaga's (63/5)/[63/41] sets[24] and for H atoms, the (4)/[4] set,[25] are used. For Mg, Huzinaga's (533/5)/[53111/311] set[24] plus two p-type polarization functions ($\zeta = 0.045$ and 0.143) and d-type polarization functions ($\zeta = 1.01$) are used. For S, Huzinaga's (533/53)/[5321/521] set[24] plus p-type anion basis ($\zeta = 0.041$) and d-type polarization function ($\zeta = 0.421$) are used. For Fe, Huzinaga's (5333/53/5)/[53321/53/41] set plus p-type basis ($\zeta = 0.082$) are used.

The effects of the proteins and waters (consisting of about 30 000 atoms) are introduced by a point charge model. The geometries of the heavy atoms in the PSRC are taken from the X-ray structure[2] (1PRC in Brookhaven Data Bank[23]). The positions of the hydrogens are estimated by using the molecular-modeling software SYBYL.[26] The published charges[27,28] are put on all the atoms of proteins and waters. The ionized form is adopted for the ionizable residues, ASP, LYS, ARG, and GLU. For the other chromophores surrounding the chromophore under consideration, the Mulliken charges calculated from the Hartree−Fock orbitals are put on the constituent atomic positions.

The polarization effect of proteins may also be important for the excited state whose dipole moment is much different from that of the ground state. It is taken into account by using the continuum model expressed by the interaction of the dipole moment μ of the molecule under consideration with the solvent reaction field, represented by the refractive index η and the effective radius of the spherical cavity a,[29,30] namely by

$$\Delta E = -\frac{\eta^2 - 1}{a^3(2\eta^2 + 1)}\langle\mu\rangle\cdot\langle\mu\rangle \qquad (2.1)$$

where ΔE is the polarization energy. We used the value of

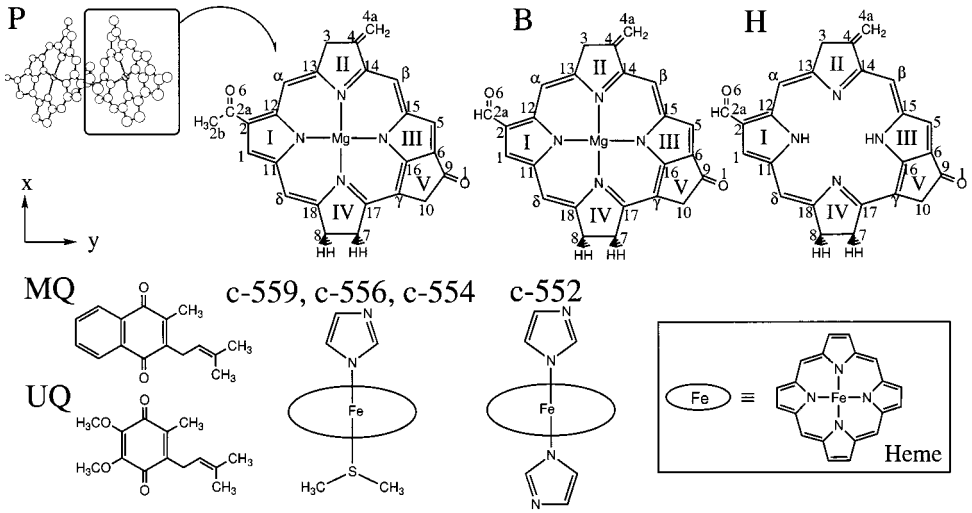

Figure 3. Calculational models for P, B, H, UQ, MQ, c-559, c-556, c-554, and c-552. For P, only monomer is shown. Some substituents were replaced by hydrogens if they do not π-conjugate with the rings. Labeling of the atoms and groups for P, B, and H is also defined.

TABLE 1: Number of MO, Active Space, Threshold, and Dimension in the SAC/SAC−CI Calculations[a]

chromophore	P	B_M	B_L	H_M	H_L	MQ	UQ	c-554	c-556	c-559	c-552
no. of MO	578	282	282	258	258	160	174	318	318	318	318
active space[b]	90 × 220 (310)	43 × 91 (134)	42 × 90 (132)	42 × 84 (126)	42 × 84 (126)	27 × 53 (80)	30 × 61 (91)	95 × 151 (246)	95 × 151 (246)	95 × 151 (246)	94 × 154 (246)
ground state											
threshold[c]	3×10^{-6}	1×10^{-5}	1×10^{-5}	1×10^{-5}	1×10^{-5}	1×10^{-5}	1×10^{-5}	2×10^{-5}	2×10^{-5}	2×10^{-5}	2×10^{-5}
dimension											
before[d]	196 049 700	7 149 870	7 661 654	6 228 684	6 228 684	1 023 165	1 677 195	102 911 030	102 911 030	102 911 030	102 911 030
after[e]	37 549	7 570	7 582	7 298	7 983	5 021	4 347	21 646	22 676	21 485	25 833
E_{corr}[f]	−0.157 52	−0.122 77	−0.115 46	−0.134 99	−0.150 73	−0.135 38	−0.887 80	−0.185 68	−0.204 48	−0.178 45	-0.252 80
excited state											
threshold[c]	2×10^{-7}	1×10^{-6}	1×10^{-6}	1×10^{-6}	1×10^{-6}	1×10^{-6}	1×10^{-6}	2×10^{-5}	2×10^{-5}	2×10^{-5}	2×10^{-5}
dimension											
before[d]	196 049 700	7 149 870	7 661654	6 228 684	6 228 684	1 023 165	1 677 195	102 911 030	102 911 030	102 911 030	102 911 030
after[e]	226 726	37 140	45 188	40 968	43 165	28 630	32 948	68 813	70 687	63 052	70 703

[a] Calculations with protein model. [b] Number of occupied MOs time the number of unoccupied MOs. The number in parentheses is the total number of active MOs. [c] Energy thresholds for the perturbation selection. [d] Number of linked operators before the perturbation selection. [e] Number of linked operators after the perturbation selection. [f] Correlation energy for the ground state in hartrees.

1.427 for η (bulk property of cyclohexane) and 6.5 Å for a.[9] The dependence on the value of η was checked by using the value for benzene, 1.498, and was confirmed to be small.

In the SAC/SAC−CI calculations, the orbitals whose energies are within −0.7 to +0.7 au are chosen for the active space, in which at least 2p electrons are correlated. From our experiences, this criteria would be enough to reproduce the low-lying excited states of the porphyrin compounds.[14−22] In Table 1, we have summarized the number of the active orbitals. For P, which is the largest molecule in the present calculation, the 90 occupied and 220 unoccupied orbitals (total 310 orbitals) are taken as active MOs from 578 SCF MOs. For the four hemes in the cytochrome *c* unit, only the inner 1s cores are taken as frozen orbitals, so that the active space is wider and the calculational accuracy is better for these hemes.

All single excitation operators are included in the linked term of the SAC/SAC−CI calculations and the perturbation selection[15,31] is carried out for double excitation operators. For the ground and excited states of the porphyrin compounds, the energy thresholds, 1×10^{-5} and 1×10^{-6} au are used, respectively. For the ground, excited, and ionized states of P, the thresholds of 3×10^{-6}, 2×10^{-7}, and 3×10^{-6} au, respectively, are used. For the hemes in cytochrome *c* unit, the threshold is 2×10^{-5}. The dimensions of the SAC/SAC−CI calculations are shown in Table 1, where the correlation energies for the ground states of these compounds are also summarized. The numbers of the doubly excited configurations are comparatively smaller than our previous calculations, because the aim of the present calculation is only for the states lower than about 3 eV. Therefore, the correlation energies calculated for these molecules are relatively small in comparison with our previous results.

For the Hartree−Fock SCF calculations, the HONDO version 8 program[32] was used and for the SAC/SAC−CI calculations, the SAC−CI 96[33] and SAC 85 programs[34] were used. Parallel computation algorithm was adopted for the integral transformation step which was the most time-consuming step in the present calculations.

We also calculated the linear dichroism (LD) spectrum for the system. The expression for the LD is given by[8]

$$|\mu|_{\perp}^2 - |\mu|_{\parallel}^2 = (1 - 3\cos^2\theta)|\mu|^2 \qquad (2.2)$$

where θ is the angle between the transition moment μ of the state and the pseudo-C_2 axis. The signs, "⊥" and "∥", denote to be perpendicular and parallel, respectively, to the pseudo-C_2 axis. The plus region corresponds to $90° > \theta > 55°$, and the minus region corresponds to $55° > \theta > 0°$.

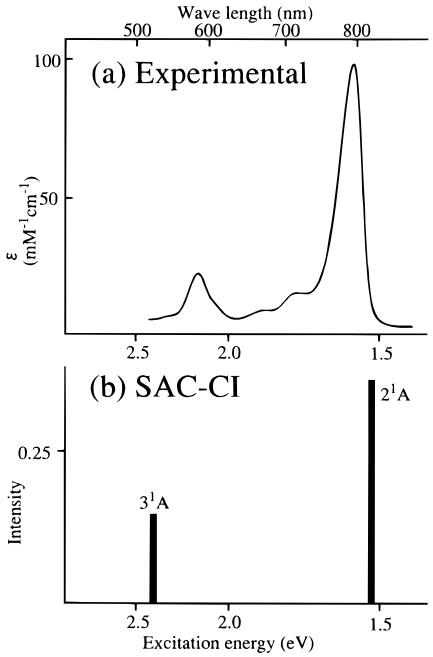

Figure 4. Electronic spectra of BChl *b* monomer. (a) Experimental absorption spectrum.[35] (b) Theoretical SAC−CI spectrum.

III. Excited States of Special Pair

The largest compound in the present calculations is the special pair, P, which is a dimer of bacteriochlorophyll *b* (BChl *b*). The ground and excited electronic structures of P are rather easily understood by comparing with those of the monomer. For this reason, we first show the results for BChl *b* monomer.

Figure 4 shows the experimental[35] and SAC−CI theoretical spectra of BChl *b* monomer, and Table 2 shows the data for the excited states. The SAC−CI results reproduce well the excitation energy and the direction of the oscillator strength observed for BChl *b* monomer. The average error in the excitation energy is 0.14 eV. The first excited state, 2^1A, is characterized as the HOMO to LUMO ($\pi-\pi^*$) excitation to which the HOMO-1 to LUMO+1 ($\pi-\pi^*$) excitation slightly mixes. In the free base porphin (FBP),[15] these HOMO to LUMO and HOMO-1 to LUMO+1 excitations were almost degenerate and their contributions to the transition moment almost canceled each other, resulting in a very small oscillator

TABLE 2: Excited States of BChl *b* Monomer Calculated by the SAC/SAC−CI Method

	SAC/SAC−CI				exptl[a]	
state	main configuration[b] ($C > 0.2$)	excitation energy (eV)	oscillator strength[c]		excitation energy[c] (eV)	
2^1A	−0.91(H→L)+0.21(H-1→L+1)	1.52	0.395	*y*	1.60	y
3^1A	−0.88(H-1→L)−0.32(H→L+1)	2.34	0.179	*x*	2.15	*x*
4^1A	−0.89(H-2→L)−0.15(H-3→L)	3.53	0.0129	*x*		

[a] Reference 35. [b] H and L denote HOMO and LUMO, respectively. [c] "*x*" and "*y*" are the directions of the transition moment which are parallel and perpendicular to the axis along the two reduced pyrrole rings.

TABLE 3: Ground and Excited States of Special Pair (P) Calculated by the SAC/SAC−CI Method

		net charge		dipole	δE_{Pol}[c]	excitation energy (eV)			
state	character[a]	P_L[b]	P_M[b]	moment (debye)	(eV)	in gas phase	in protein A[d]	in protein B[e]	exptl[f]
X^1A		−0.075	0.075	5.45					
2^1A	Ex	−0.179	0.179	3.60	+0.01	1.42	1.40	1.41	1.25 (I)
3^1A	Ex	−0.019	0.019	7.55	-0.01	1.63	1.62	1.61	1.46 (II)
4^1A	Ex	−0.197	0.197	5.75	0.00	2.18	2.10	2.10	1.88 (VII)
5^1A	CT	−0.674	0.674	18.00	-0.05	2.22	2.37	2.31	
6^1A	CT	0.506	−0.506	22.25	-0.22	2.52	2.57	2.35	
7^1A	Ex	0.043	−0.043	8.48	-0.02	2.61	2.48	2.46	2.23 (XI)
8^1A	CT	−0.675	0.675	16.65	-0.10	3.15	2.96	2.86	
9^1A	CT	0.539	−0.539	20.00	-0.18	3.34	3.37	3.19	

[a] Ex and CT denote exciton and charge-transfer excited states, respectively. [b] P_L and P_M denote bacteriochlorophyll monomer constructing P. [c] Change in the excitation energy due to the polarization effect of proteins. [d] Excitation energy including protein effect represented by the point-charge electrostatic model. [e] Excitation energy including protein effect represented by the point-charge electrostatic model plus continuum model. [f] Reference 5.

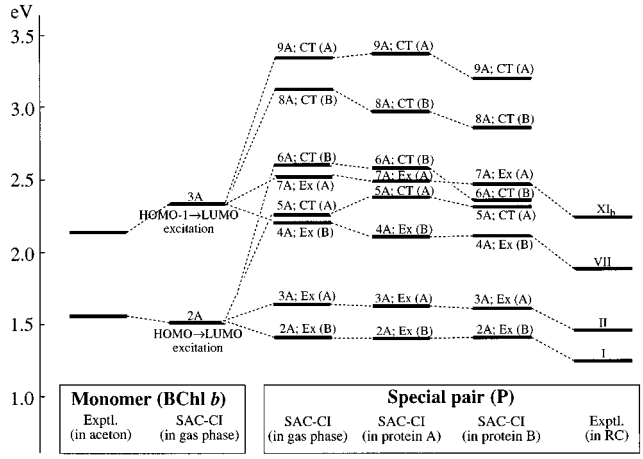

Figure 5. Energy levels of the excited states of BChl *b* monomer and dimer (special pair P) calculated by the SAC−CI method compared with the experiments.[5,35] Ex and CT denote exciton and charge transfer states, respectively, and A and B in the parentheses denote the symmetry representations to which the excited states of P approximately belong.

strength.[21,36] In the case of BChl *b*, the reductions of the double bonds in the pyrrole rings cause a destabilization of the HOMO-1 and LUMO+1 energy levels, resulting in a breakdown of the quasidegeneracy, which leads to a larger intensity than that of FBP. The second excited state, 3^1A, is characterized as HOMO-1 to LUMO ($\pi-\pi^*$) excitation. The directions of the transition moments of the 2^1A and 3^1A states are perpendicular and parallel, respectively, to the axis along the two reduced pyrrole rings.

The electronic structures of the ground and excited states of P are easily understood by comparing with those of the monomer. In Figure 5, the calculated lower excited states of P are compared with those of the monomer, BChl *b*. We see that each monomer state splits into four by dimerization: two exciton (Ex) states and two charge-transfer (CT) states. The dotted lines from the monomer to the dimer show this splittance. The two Ex states are lower than the two CT states. Thus, the two Q states (2 and 3^1A states) of the monomer split into eight states (four Ex and four CT states) in the dimer P.

The first excited state of P, the 2^1A state, is calculated at 1.40 eV and shows a red shift caused by the dimerization. A reason of the red shift is that the HOMO−LUMO energy gap decreases by the dimerization due to the HOMO−HOMO and LUMO−LUMO interactions between the two monomers. Table 3 shows the amount of charge transfer in the ground and excited states of P. In the ground state, P_L is slightly negative, while P_M is slightly positive. In the excited states, the CT state is clearly characterized by a large amount of charge transfer, giving a large dipole moment. This polarized electronic structure of the CT state would cause a large geometric relaxation of P in the CT excited state.

Table 3 and Figure 5 shows the effects of the proteins on the excitation energy, but they are discussed in a later section.

IV. Assignment of the Excitation Spectrum of the PSRC

The absorption and the LD spectra of the PSRC of *Rps. viridis* observed by Breton[5] and those calculated by the SAC−CI method are compared in Figure 6. These spectra were redrawn from those in Figure 2 such that the horizontal axes are given in eV. The experimental absorption spectrum has at least fourteen peaks in the energy range of 1.25−2.5 eV. As in Figure 2, the experimentally observed peaks in the absorption spectrum are numbered from I to XIV and the dotted lines show the present assignments. The excitation energy, oscillator strength, and the LD data, which is the angle of the transition moment from the C_2 axis, are shown in Table 4. The present assignments are carried out based on the excitation energy, oscillator strength, LD data, and other experimental information available. The average discrepancy from the experimental peak positions is 0.13 eV.

The first band I at 1.25 eV has been attributed to the Q_y state of P, since no such low-lying peak exists in the experimental absorption spectra of B and H monomers (see Table 2, for example), and since the PSRC including P^+ (chemically oxidized) does not have this peak.[5] In the present calculation,

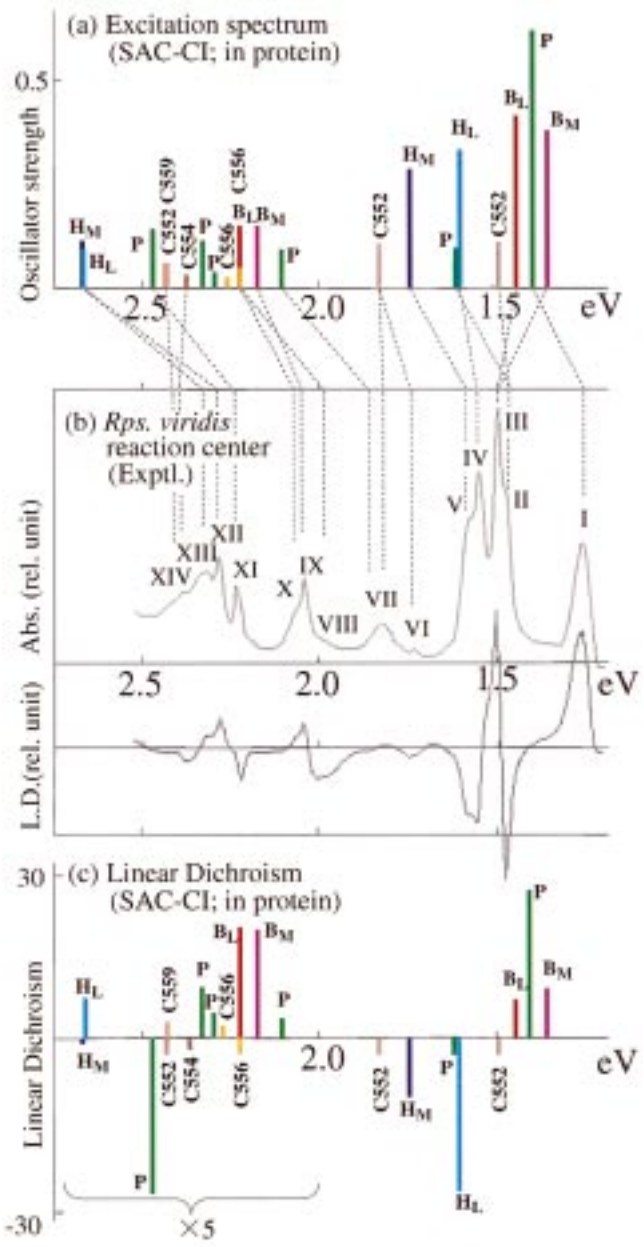

Figure 6. Absorption and linear dichroism spectra of the PSRC. (a) SAC−CI theoretical excitation spectrum. (b) Experimental absorption and linear dichroism spectra.[5] (c) SAC−CI theoretical linear dichroism spectrum.

the peak positions of the $B_M(2^1A)$ and $P(2^1A)$ states are calculated at 1.35 and 1.41 eV, respectively. As for the peak position, the $B_M(2^1A)$ state is closer to the experimental value, while for the oscillator strength and LD data, the $P(2^1A)$ state is closer to the experimental values. We think that the experimental data for the PSRC including P^+ is decisive and therefore assign $P(2^1A)$ state to Band I of the experimental spectrum.

The main configuration of $P(2^1A)$ state consists of HOMO-(H) to LUMO(L) ($\pi-\pi^*$) excitation with a small mixing of H-1 to L+1 excitation. As seen in Table 3, the $P(2^1A)$ state is characterized as an exciton (Ex) state where the two Q_y states (H→L excitation) of the monomers couple and, therefore, belongs to the B symmetry of the pseudo-C_2 symmetry of the special pair. The calculated intensity 0.607 is about twice as large as that of the monomer 0.395, which is already large owing to the partial hydrogenation of the porphyrin double bond as shown in the preceding section. This enhancement is due to the Ex character of the state; the additive contribution of the intensities of the two monomers. It is noteworthy that this strong intensity has an important biological implication in the photoexcitation process of the PSRC. Compared with the ground-state $P(X^1A)$ of special pair, about 0.1 electron is transferred from P_M to P_L as seen in Table 3, so that $P(2^1A)$ state has a small CT character.

Band II at 1.46 eV is observed as a red-shifted shoulder of an intense band III.[5] This peak has been attributed to the excited state of P, since it vanishes in the absorption spectrum of P^+ of the oxidized PSRC shown in the lower part of Figure 2.[5] In the oxidized state, not only P but also the hemes in the cytochrome unit are oxidized. Therefore, we propose here that this band II consists of two states, II_a and II_b, which are the first excited state of the c-552 heme calculated at 1.50 eV and the $P(3^1A)$ state calculated at 1.61 eV. We propose this assignment by the following reasons. First, band II disappears for the PSRC including P^+, so that the candidates are P and hemes. Second, comparing the spectra of the PSRC's of *Rps. viridis* and *Rb. sphaeroides* given by Breton,[5] we notice that the intensity of the LD spectrum of peak II is stronger in the former than in the latter. This may indicate that peak II of *Rps. viridis* consists of two states, while that of *Rb. sphaeroides* consists of one state. Due to our SAC−CI calculations, the first excited state of c-552 is at 1.53 eV with the oscillator strength of 0.124 (stronger) and with the LD angle of 43.3°, while the $P(3^1A)$ state is at 1.61 eV with the oscillator strength of 0.09 (weaker) and the LD angle of 36.9° inconsistent with the observed peak position at 1.46 eV and the large negative LD peak whose angle was estimated to be about 30°.[5] Further, the energy separation between the first and second excited states of P are 0.20 eV by SAC−CI which is comparable with the experimental value 0.21 eV.

The main configuration of $P(3^1A)$ state is H-1 to L ($\pi-\pi^*$) excitation with a small in-phase mixing of H to L+1 excitation, which is characterized as an exciton coupling of the monomer Q_y states (H to L excitation). The intensity of this state is much smaller than that of $P(2^1A)$ state, though these two states are both Ex states. The reason is that, in the dimer of pseudo-C_2 symmetry, the $P(3^1A)$ state belongs to the A symmetry in which the transition from the ground state is allowed only along the direction along the C_2 axis, but the H to L excitation of the monomer has only a small intensity component in this direction.

The next very strong peak centered at 1.49 eV, band III, also seems to be composed of the two states: a stronger peak with the LD angles θ of about 70° and a weaker shoulder peak in higher energy with a smaller LD angle. We designate these two peaks as peak III_a and III_b, respectively. Both of these peaks still exist in the spectrum of the oxidized PSRC, and therefore they should originate from either B or H. We assign peaks III_a and III_b to the first excited Q_y states of B_M and B_L, respectively, since they are calculated at 1.35 and 1.45 eV, respectively, and since the calculated LD angles 67.2° and 64.3° for B_M and B_L, respectively, are close to the experimentally observed values.

We assign bands IV (1.54 eV) and V (1.57 eV) to the first excited states of H_L (2^1A) and H_M (2^1A) calculated at 1.59 and 1.75 eV, respectively. These states originate from the Q_y state of H whose main configuration is H to L ($\pi-\pi^*$) excitation. This assignment is supported from both the oscillator strength and the θ value of the LD spectrum. The peak IV is stronger than the peak V, but both are weaker than band III. Correspondingly, the calculated oscillator strengths are 0.323 and 0.283 for $H_L(2^1A)$ and $H_M(2^1A)$, respectively, but they are

TABLE 4: Singlet Excited States of Chromophores in the Photosynthetic Reaction Center of *Rhodopseudomonas Viridis*

	SAC−CI (gas phase)			SAC−CI (in protein)						exptl.[f]			
chromophores[a]	state	excitation energy (eV)	oscillator strength	state	main configuration[b] ($\|C\| \geq 0.3$)	excitation energy[c] (eV)	energy shift[d] (eV)	oscillator strength	linear dichroism (deg)[e]	excitation energy (eV)	(nm)	(peak)	linear dichroism (deg)[e]
P	2^1A	1.42	0.673	2^1A	0.88(H→L)	1.41	−0.01	0.607	85.1	1.25	990	(I)	90
c-552	2^1A	1.53	0.160	2^1A	−0.66(H-1 →L)+0.57(H→L)	1.50	−0.03	0.124	43.3	1.46	850	(II_a)	30
P	3^1A	1.63	0.067	3^1A	−0.85(H-1 →L)	1.61	−0.02	0.090	36.9	1.46	850	(II_b)	30
B_M	2^1A	1.42	0.335	2^1A	−0.92(H→L)	1.35	−0.07	0.363	67.2	1.49	834	(III_a)	70
B_L	2^1A	1.52	0.372	2^1A	0.92(H→L)	1.45	−0.07	0.406	64.3	1.49	834	(III_b)	70
H_L	2^1A	1.65	0.317	2^1A	−0.87(H→L)−0.34(H-1 →L+1)	1.59	−0.06	0.323	33.7	1.54	805	(IV)	40
H_M	2^1A	1.67	0.284	2^1A	−0.87(H-1 →L)	1.75	+0.08	0.283	28.6	1.57	789	(V)	40
c-552	3^1A	1.82	0.013	3^1A	0.68(H→L)+0.56(H-1 →L+1)	1.83	+0.01	0.110	38.3	1.75	709	(VI)	
										1.81	684	(VII)	
P	4^1A	2.18	0.100	4^1A	−0.89(H-2 →L)	2.10	−0.08	0.088	61.0	1.88	660	(VII)	
c-556	2^1A	2.26	0.034	2^1A	-0.58(H→L)−0.42(H-1 →L+1)	2.23	−0.03	0.047	44.6	1.99	615	(VIII)	30
B_M	3^1A	2.32	0.125	3^1A	0.88(H-1 →L)	2.17	−0.15	0.149	79.8	2.04	607	(IX)	70
B_L	3^1A	2.41	0.140	3^1A	-0.87(H-1 →L)−0.30(H-1 →L+1)	2.23	−0.18	0.148	77.1	2.06	600	(X)	70
c-556	3^1A	2.30	0.023	3^1A	-0.71(H→L+1)+0.49(H-1 →L)	2.27	−0.03	0.020	62.2				
P	5^1A	2.22	0.070	5^1A	−0.88(H→L+1)	2.31	+0.09	0.038	87.4				
P	6^1A	2.52	0.083	6^1A	−0.83(H-1 →L+1)	2.35	−0.17	0.120	71.5				
P	7^1A	2.61	0.181	7^1A	0.70(H-3 →L)−0.37(H-2 →L+1)	2.46	−0.15	0.144	25.3	2.23	556	(XI_b)[g]	30
H_L	3^1A	2.67	0.103	3^1A	-0.84(H-1 →L)−0.44(H-1 →L+1)	2.66	−0.01	0.091	61.6	2.28	544	(XII)	70
H_M	3^1A	2.67	0.090	3^1A	0.82(H-1 →L)+0.47(H-1 →L+1)	2.67	0.00	0.113	53.6	2.32	534	(XIII)	70
c-554	2^1A	2.40	0.036	2^1A	0.80(H→L)−0.50(H-1 →L+1)	2.38	−0.02	0.035	46.1	2.36	525	(XVI_a)	
c-559	2^1A	2.45	0.014	2^1A	0.81(H→L)+0.45(H-1 →L+1)	2.44	−0.01	0.058	64.1				
c-552	6^1A	2.46	0.150	6^1A	0.77(H-2 →L)+0.47(H-3 →L)	2.44	−0.02	0.059	45.4	2.38	520	(XVI_b)	
UQ	2^1A	3.85	0.018	2^1A	0.92(H→L)	2.86	−1.01	0.001	76.8				
P	8^1A	3.15	0.006	8^1A	0.80(H-2 →L+1)+0.38(H-3 →L)	2.86	−0.29	0.013	35.6				
P	9^1A	3.34	0.009	9^1A	0.78(H-3 →L+1)+0.37(H-3 →L)	3.19	−0.15	0.018	84.7				
MQ	2^1A	3.52	0.000	2^1A	0.74(H-4 →L)+0.45(H→L)	3.44	−0.08	0.002	58.0				

[a] P, B, and H denote special-pair, bacteriochlorophyll, and bacteriopheophytin, respectively. L and M denote L- and M-branches, respectively. [b] H and L denotes HOMO and LUMO, respectively. [c] Excitation energy including protein effect by a point charge electrostatic model. For P, the polarization effect of protein is also included by a contiuum model. [d] Energy shift in excitation energy between in protein and in gas phase. Plus and minus signs denote blue and red shifts, respectively. [e] Angle of the transition moment vector with the pseudo-C_2 axis of the reaction center. [f] Reference 5. [g] For peak XI_a, see text.

smaller than those of $B_M(2^1A)$ and $B_L(2^1A)$, 0.363 and 0.406, respectively. The calculated LD angles are 33.7° for H_L and 28.6° for H_M, which correspond well with the experimental angles around 40° for both, large negative values in the LD spectrum.[5] The present result supports the energetic order of H_L and H_M proposed previously,[37] and this order is considered to be due to the difference in molecular geometry between H_L and H_M since the gas phase result shown in Table 4 shows the same order of the states as that in protein. Note, however, that the protein effect enlarges the difference. This assignment is consistent with the experimental result that an illumination of $\lambda > 900$ nm light to the PSRC bleached these peaks due to the photoreduction of the L-branch chromophores.[37] Last, we note that the spectrum of *Rb. sphaeroides* is somewhat different from the present spectrum: there is only one strong band in this region in contrast to the present two bands. This is perhaps due to the differences in the geometry of H_L and H_M and in the protein environment between these two PSRCs.

A small peak VI, is observed at 1.75 eV in the absorption spectrum and its LD has a negative contribution as seen from Figure 6. To the best of our knowledge, no assignment has been made for this peak. Actually, the assignment of this peak is rather difficult, since the peak itself is so weak and it seems to exist also in the absorption spectrum of the chemically oxidized PSRC (Figure 2).[5] In our present SAC−CI calculation, the second excited state (3^1A) of c-552 is calculated at 1.83 eV with a negative LD component. Though this result well accounts for the spectrum of the reduced PSRC, it may contradict with the spectrum of the oxidized one. Maybe we have to perform calculations for the excited states of the cations of P and the hemes in the c-type cytochrome unit for the final assignment. We note that, in the level of the Koopmans theorem, the third excited state of $c\text{-}552^+$ is calculated to be 1.91 eV, which might explain this peak still existing in the spectrum of the oxidized PSRC.

Band VII is composed of at least two states from the LD spectrum.[5] A peak at 1.81 eV was proposed to be assigned to H_L anion, since the intensity of this peak increase in the absorption spectrum of the photoreduced PSRC.[37] We therefore calculated the electron attached states of H_L and obtained the excitation energy for X^2A to 2^2A (L to L+1) transition at 1.4 eV. The discrepancy of 0.4 eV is somehow large and probably due to a geometric relaxation of the ground state of the anion, which was not taken into account in this calculation. Further, we note that the intensity of this band decreases when the PSRC is chemically oxidized.[5] Then, the second excited state (3^1A) of c-552 calculated at 1.83 eV may also be assigned to this band: this is another possible assignment of $c\text{-}552(3^1A)$.

A blue-side shoulder (1.88 eV) of band VII was proposed to be a Q_x component of P from the circular dichroism (CD) spectra of the oxidized PSRC.[5] We attribute $P(4^1A)$ state calculated at 2.10 eV to this shoulder. The calculated LD data shows a small plus, which is consistent with the experimental one shown in Figure 6. The energy separations from the first singlet excited state of P in the theory and experiment[5] are 0.70 and 0.63 eV, respectively, which are close. The $P(4^1A)$ state is certainly classified to the Q_x component, since the main configuration of the state, H-2 to L ($\pi-\pi^*$) excitation, originates from the monomer 3^1A state, H-1 to L excitation.

Band VIII at about 1.99 eV is a featureless red-side shoulder of band IX. The LD experiment showed a characteristic large negative component as seen in Figure 6 ($\theta \simeq 30°$).[5] Breton assigned band VIII to P and the consistent assignment would be $P(7^1A)$ state calculated at 2.46 eV. Although the discrepancy of the peak position from the experiment, 0.44 eV, is very large, the calculated small angle (25.3°) is close to the

experiment.[5] Another assignment of band VIII is 2^1A state of c-556 calculated at 2.23 eV (just at 556 nm), which also has a small calculated LD angle of 44.6°. The discrepancy here is 0.21 eV. Both of these assignment is consistent with the fact that band VIII disappears when the PSRC is oxidized.[5] We prefer the second assignment since the discrepancy is smaller and since the P(7^1A) state is preferentially assigned to band XI at 2.23 eV (556 nm) whose LD angle was also observed to be small (30°).

The band IX and X observed at 2.04 and 2.07 eV are attributed to the Q_x states of B_M(3^1A) and B_L(3^1A) calculated at 2.17 and 2.23 eV, respectively. The present assignment to the Q_x states is consistent with the previous ones,[5,37] but Breton assigned B_L, to band IX in contrast to the present assignment. Experimentally, the LD angle is around 70° but it is larger for band IX than for band X and this is reproduced by the present assignment. The energy ordering of the Q_x states of B_L and B_M calculated in protein is the same as that in a gas phase, which indicates that the different molecular structures of B_L and B_M are the origin of the ordering of the states.

In the blue shoulder region of band X, some states may exist (Figure 6) and c-556(3^1A), P(5^1A), and P(6^1A) states were obtained in our calculation. The intensities of these states are smaller than those of the Q_X states of B_M and B_L, and they should give positive contribution to the LD spectrum. This assignment has some support from the experiment, since the bands IX and X of the oxidized PSRC involving P^+ have smaller intensity than those of the reduced PSRC.[5] The main configuration of P(5^1A) and P(6^1A) states are H to L+1 and H-1 to L ($\pi-\pi^*$) excitations, respectively, which are the CT coupling between monomer Q_x states. Net charges shown in Table 3 clearly show their CT character; 0.67 and 0.51 electrons are transferred from P_M to P_L and from P_L to P_M, respectively. The P(6^1A) state has relatively large intensity in comparison with other CT states: it borrows its intensity from the Ex state (2^1A) through a configuration mixing.

Bands XI observed at 2.23 eV (556 nm) was attributed to heme c-559.[5] However, band XI would have two components, since the sharp peak (XI_b) vanishes and a shoulder (XI_a) remains in the absorption spectrum of the oxidized state (P^+).[5] The sharp one has a characteristic large negative LD. We assign P(7^1A) state to this sharp component, since our SAC−CI calculation gives very small LD angle (25.3°) and a large oscillator strength to this state. P(7^1A) state has the main configuration characterized by H-3 to L ($\pi-\pi^*$) excitation, and is classified as the Q_x component of the excited state of P, since this transition originates from the monomer H-1 to L excitation. In the present calculation, the first excited state of c-556(2^1A) calculated at 2.23 eV (556 nm) with a small negative LD value has been assigned to band VIII. The first excited state of c-559 (2^1A), which was experimentally assigned to band XI, is calculated at higher energy, 2.44 eV, with a plus LD contribution and with a small oscillator strength (0.058). It is assigned in the present calculation to a component of peak XVI, as discussed below. For the shoulder of the band XI, which still exists in the oxidized states, the excited states of hemes in their oxidized states might be the origin, since they are produced by the chemical oxidation.[5] Here, c-559^+ is certainly the most probable origin since it has an excitation energy at 2.25 eV estimated at the level of the Koopmans theorem. Other calculated excitation energies of the heme cations in this energy region are 2.44 and 2.55 eV for c-552^+, 2.34 and 2.57 eV for c-554^+, 2.49 and 2.67 eV for c-556^+, and 2.45 eV for c-559^+.

Band XII and XIII observed at 2.28 and 2.32 eV are attributed to the Q_X states of H_L and H_M, respectively. The illuminated result[37] indicated this energy order. Our result is 2.66 eV for H_L and 2.67 eV for H_M, and the energy splitting is obtained as the protein effect: the gas-phase energy levels of H_L and H_M are the same. This ordering is also supported by the calculated LD angles: the angle of the lower energy state is larger than that of the higher energy state in accordance with the LD spectrum shown in Figure 5.

The excited states of the hemes, c-554(2^1A), c-559(2^1A), and c-552(6^1A) are calculated at 2.38, 2.44, and 2.44 eV, respectively. Their characters are H to L, H to L, and H-2 to L excitations, respectively, and c-554(2^1A) and c-552(6^1A) have negative LD components. In the experimental spectrum, we observe a negative LD region, band XIV, at the blue-side shoulder of band XIII, and at 2.36 and 2.38 eV we see small peaks having negative LD components. We therefore assign c-554(2^1A) and c-552(6^1A) states, respectively, to these peaks. The LD angle of c-554(2^1A) is a bit larger than that of c-552(6^1A), in accordance with experiment.

In the energy region higher than 2.7 eV, four excited states UQ(2^1A), P(8^1A), P(9^1A), and MQ(2^1A) are calculated by the SAC−CI method, but all the states have very small intensities. P(8^1A) and P(9^1A) states calculated at 2.96 and 3.37 eV are intramolecular CT states as shown in Table 3. UQ(2^1A) state calculated at 2.86 eV is H to L ($\pi-\pi^*$) excitation. Note a very large protein effect on this state which is discussed below. MQ(2^1A) state calculated at 3.44 eV is n−π^* excited state with which H to L ($\pi-\pi^*$) excitation strongly mixes.

V. Protein Effect on the Excited States

In the present SAC−CI calculations of the ground and excited states of the chromophores, the proteins, waters, and the other chromophores involved in the PSRC were represented by the point charge model. For P, we further considered the polarization effect of the protein medium as shown in Table 3. In Table 4, the excitation energies and the oscillator strengths of the chromophores calculated in the gas phase are compared with those calculated in the environment of the proteins. The geometries of the chromophores are the X-ray structures, also common for both gas-phase and in-protein calculations. Table 4 also shows the energy shift caused by the protein environment. Almost all the states are red shifted by an inclusion of the protein effect, though some states, P(5^1A) state in particular, are blue shifted. The calculated energy shifts are less than 0.2 eV, except for UQ, since the orbital-energy gaps are not so much affected by the protein potential.

For UQ, the excitation energy is red shifted by as large as 1.01 eV by the proteins, since the HOMO is more largely destabilized by the protein potential than the LUMO. The energy shifts of the HOMO and LUMO are +1.73 and +0.79 eV, respectively. The reason of a larger shift of the HOMO is that the orbital has a large amplitude in the negative-potential region generated by GLU L 212. Unfortunately, the excitation peak of UQ is not identified in the experimental spectrum, since the absorption band of UQ must be hidden by the strong broad bands composed of the Soret bands of the porphyrins.

The excitation energy shifts of B's are relatively large in comparison with those of the other chromophores. Parson et al.[38] compared the absorption spectra of the RC and bacteriochlorophyll *b* in ether solvent and observed red shifts of the Q_y and Q_x bands. The present calculation gave the red shifts of −0.07 eV for the Q_y bands of B_L and B_M and −0.15 and −0.18

eV for the Q_x bands of B_L and B_M, respectively, which are comparable with the experimental values, −0.11 eV for the Q_y bands of B's, −0.11 eV for the Q_x bands of B_M, and −0.08 eV for the Q_x bands of B_L.[5,35] The reason of the red shift is accounted for by the orbital-energy change as in UQ. The Q_y and Q_x bands of B's are due to the HOMO to LUMO and HOMO-1 to LUMO excitations, respectively. The orbital energies of B_L and B_M are destabilized by the negative electrostatic potentials due to ASP M 182 and ASP L 155, respectively. But, the energy shifts of the LUMO's for B_L and B_M are smaller than those of the HOMO's and HOMO-1's by about 0.2 eV, since the LUMO regions are more distant from this negative potential region in both B_L and B_M.

The oscillator strengths are also affected by the protein environment, but the effects are not monotonic as seen from Table 4: some peaks become more intense but the others become less intense. The effects are not small, as expected, because the oscillator strengths of the porphyrins are generally the results of the two large canceling contributions.[21,36]

For P, we have considered the effect of proteins expressed by the point-charge model and the polarization model and the results are shown in Table 3 and Figure 5. As seen from these results, the polarization effect is very small for the Ex states, since the induced dipole moments are small. For this reason, the polarization effects were calculated only for P. A remarkably large polarization effect is seen for $P(6^1A)$ state which becomes lower than $P(7^1A)$ states after the polarization effect is included: otherwise the ordering of $P(6^1A)$ and $P(7^1A)$ states are reversed. $P(6^1A)$ state is the CT state and therefore is much stabilized by the polarization effect.

VI. Summary and Conclusion

The excitation spectrum of the PSRC of *Rps. viridis* has at least 14 distinct bands in a narrow energy range from 1.25 to 2.4 eV. We calculated the excitation spectrum and the LD spectrum of this PSRC theoretically by the SAC−CI method and gave the assignment of all the peaks. We used the excitation energy, oscillator strength, LD angle, and other information available. In particular, the comparisons with the spectra of the chemically oxidized PSRC, in which P and hemes are oxidized, and of the PSRC of *Rb. sphaeroides* were very useful.

Our final assignment is summarized in Table 4 and Figure 6. Band I at 1.25 eV(990 nm) is assigned to $P(2^1A)$ Q_Y state. Band II at 1.46 eV(850 nm) is considered to be composed of the Q_Y states of c-552 and $P(3^1A)$. Band III at 1.49 eV (834 nm) consists of the two states, $B_M(2^1A)$ and $B_L(2^1A)$, and bands IV and V at 1.54 eV (805 nm) and 1.57 eV (789 nm) are assigned to $H_L(2^1A)$ and $H_M(2^1A)$ state, respectively. The c-552(3^1A) state may be assigned to a small peak VI at 1.75 eV (709 nm) or to peak VII at 1.81 eV (684 nm), though the main peak at 1.81 eV is due to H^-. Band VII at 1.85 eV (660 nm) is assigned to $P(4^1A)$ Q_X state. Band VIII at 1.99 eV (615 nm) has a negative LD component and disappears by chemical oxidation and assigned to c-556(2^1A) state, different from the assignment to $P(7^1A)$ state. Band IX and X at 2.04 eV (607 nm) and 2.06 eV (600 nm) are assigned to $B_M(3^1A)$ and B_L-(3^1A). Band XI at 2.23 eV (556 nm) has a large negative LD peak and is assigned to $P(7^1A)$ having a small LD angle θ. The c-556(3^1A) state also composes this peak. Band XII and XIII at 2.28 eV (544 nm) and 2.32 eV (534 nm) are due to $H_L(3^1A)$ and $H_M(3^1A)$. The small peaks XIV_a and XIV_b having negative LD components at 2.36 eV (525 nm) and 2.38 eV (520 nm) are assigned to c-554(2^1A) and c-552(6^1A) state. The c-559-(2^1A) state also exists in this peak XIV. Some other states not included in the above descriptions exist, and compose the shoulders, etc., of the main peaks. The average discrepancy between the calculated and experimental excitation energies is 0.13 eV.

The protein effect on the excitation energy is calculated to be red-shifts in most cases. Although we have replaced the effects of proteins, waters and the interchromophore interactions by the classical Coulombic interactions, the calculations reproduced the experimental values rather well, which might indicate the adequacy of our model. However, a precise examination for the protein effect is very much desirable and should be considered by a more accurate treatment of protein molecules, which will be studied in the next stage.

The calculations of the ground and excited states of all the chromophores in the PSRC of *Rps. viridis* have thus made successfully by the SAC/SAC−CI method and gave a firm basis for the assignments of the experimental spectrum observed by Breton.[5] We believe that the present assignment would offer a good starting basis for a future development in the chemistry and biochemistry of the PSRC.

In the succeeding paper,[39] we study the mechanism and the unidirectionality of the electron transfer in the PSRC of *Rps. virides* using the SAC/SAC−CI wave functions of the chromophores calculated in this and the succeeding studies.

Acknowledgment. We thank Prof. K. Miki in the Faculty of Science, Kyoto University for the information on the oxidation state of the hemes. This study was supported in part by a Grant-in-Aid for Scientific Research from the Japanese Ministry of Education, Science, Culture, and Sports, and by the New Energy and Industrial Technology Development Organization (NEDO). One of the authors (J. H.) gratefully acknowledges the Research Fellowship from the Japan Society for the Promotion of Science for Young Scientists.

References and Notes

(1) Voet, D.; Voet, J. G. *Biochemistry*; 2nd ed.; John Wiley & Sons: New York, 1995; Chapter 22.

(2) Deisenhofer, J.; Epp, O.; Miki, K.; Huber, R.; Michel, H. *J. Mol. Biol.* **1984**, *180*, 385.

(3) Hörber, J. K. H.; Göbel, W.; Ogrodnik, A.; Michel-Beyerle, M. E.; Knapp, F. W. In *Antennas and Reaction Centers of Photosynthetic Bacteria*; Michel-Beyerle, M. E., Ed.; Springer-Verlag: Berlin, 1985; pp 292.

(4) Hörber, J. K. H.; W. Göbel; Ogrodnik, A.; Michel-Beyerle, M. E.; Cogdell, R. J. *FEBS Lett.* **1986**, *198*, 268.

(5) Breton, J. *Biochim. Biophys. Acta* **1985**, *810*, 235.

(6) van Stokkum, I. H.; Beekman, L. M. P.; Jones, M. R.; van Brederode, M. E.; van Grondelle, R. *Biochemistry* **1997**, *36*, 11360.

(7) van Brederode. M. E.; Jones, M. R.; van Mourik, F.; van Stokkum, I. H.; van Grondelle, R. *Biochemistry* **1997**, *36*, 6855.

(8) Parson, W. W.; Warshel, A. *J. Am. Chem. Soc.* **1987**, *109*, 6152.

(9) Thompson, M. A.; Zerner, M. C. *J. Am. Chem. Soc.* **1992**, *113*, 8210. Also see: Thompson, M. A.; Zerner, M. C., Fajar, J. *J. Am. Chem. Soc.* **1991**, *112*, 5693.

(10) Scherer, O. J.; Scharnagl, C.; Fischer, S. F. *Chem. Phys.* **1995**, *197*, 333.

(11) Nakatsuji, H.; Hirao, K. *J. Chem. Phys.* **1978**, *68*, 2053.

(12) Nakatsuji, H. *Chem. Phys. Lett.* **1978**, *59*, 362; **1989**, *67*, 329; **1989**, *67*, 334.

(13) Nakatsuji, H. *Acta Chim. Hung.* **1992**, *129*, 719.

(14) Nakatsuji, H. In *Computational Chemistry, Reviews of Current Trends*; Leszczynski, J., Ed.; World Scientific: Singapore, 1996; Vol. 2, pp 62−124.

(15) Nakatsuji, H.; Hasegawa, J.; Hada, M. *J. Chem. Phys.* **1996**, *104*, 2321; Tokita, Y.; Hasegawa, J.; Nakatsuji, H. *J. Phys. Chem. A* **1998**, *102*, 1843.

(16) Hasegawa, J.; Hada, M.; Nonoguchi, M.; Nakatsuji, H. *Chem. Phys. Lett.* **1996**, *250*, 159.

(17) Nakatsuji, H.; Hasegawa, J.; Ueda, H.; Hada, M. *Chem. Phys. Lett.* **1996**, *250*, 379.

(18) Nakatsuji, H.; Tokita, Y.; Hasegawa, J.; Hada, M. *Chem. Phys. Lett.* **1996**, *256*, 220.

(19) Tokita, Y.; Nakatsuji, H. *J. Phys. Chem. B.* **1997**, *101*, 3281.

(20) Hasegawa, J.; Ozeki, Y.; Ohkawa, K.; Hada, M.; Nakatsuji, H. *J. Phys. Chem. B* **1998**, *102*, 1320.

(21) Toyota, K.; Hasegawa, J.; Nakatsuji, H. *J. Phys. Chem. A* **1997**, *101*, 446.

(22) Nakatsuji, H.; Hasegawa, J.; Ohkawa, K. *Chem. Phys. Lett.* **1998**. In press.

(23) Abola, E. E.; Bernstein, F. C.; Bryant, S. H.; Koetzle, T. F.; Weng, J. Protein Data Bank. In *Crystallographic Databases-Information Content, Software Systems, Scientific Applications*; Allen, F. H., Bergerhoff, G., Sievers, R., Eds.; Data Commission of the International Union of Crystallography: Chester, 1987; pp 107−132. Bernstein, F. C.; Koetzle, T. F.; Williams, G. J. B.; Meyer, E. F., Jr.; Brice, M. D.; Rodgers, J. R.; Kennard, O.; Shimanouchi, T.; Tasumi, M. The Protein Data Bank: a Computer-based Archival File for Macromolecular Structures. *J. Mol. Biol.* **1977**, *112*, 535.

(24) Huzinaga, S.; Andzelm, J.; Klobukowski, M.; Radzio-Andzelm, E.; Sakai, Y.; Tatewaki, H. *Gaussian Basis Set for Molecular Calculations*; Elsevier: NewYork, 1984.

(25) Huzinaga, S. *J. Chem. Phys.* **1965**, *42*, 1293.

(26) *SYBYL*, Version 6.1;TRIPOS, Inc.: St. Louis, Missouri.

(27) Cornell, W. D.; Cieplak, P.; Bayly, C. I.; Gould, I. R.; Merz, K. M.; Freguson, D. R.; Spellmeyer, D. C.; Fox, T.; Caldwell, J. W.; Kollman, P. A. *J. Am. Chem. Soc.* **1995**, *117*, 5179.

(28) Jorgensen, W. L.; Chandrasekhar, J.; Madura, J. D.; Impey, R. W.; Klein, M. L. *J. Chem. Phys.* **1983**, *79*, 926.

(29) Karelson, M. K.; Zerner, M. C. *J. Phys. Chem.* **1992**, *96*, 6949.

(30) Onsanger, L. *J. Am. Chem. Soc.* **1936**, *58*, 1486.

(31) Nakatsuji, H. *Chem. Phys.* **1983**, *75*, 425.

(32) Dupuis, M.; Farazdel, A. *MOTECC-91*; Center for Scientific and Engineering Computations: IBM Corporation, 1991.

(33) Nakatsuji, H.; Hada, M.; Ehara, M.; Hasegawa, J.; Nakajima, T.; Nakai, H.; Kitao, O.; Toyota, K. SAC/SAC−CI program system (SAC−CI96) for calculating ground, excited, ionized, and electron attached states and singlet to septet spin multiplicities, 1998. To be submitted for publication.

(34) Nakatsuji, H. Program system for SAC and SAC−CI calculations. Program Library No. 146(Y4/SAC); Data Proccessing Center of Kyoto University: Kyoto, 1985; *Program Library SAC85*, No. 1396; Computer Center of the Institute for Molecular Science; Okazaki, 1986.

(35) Scherz, A.; Parson, W. W. *Biochim. Biophys. Acta* **1984**, *766*, 653.

(36) Toyota, K.; Hasegawa, J.; Nakatsuji, H. *Chem. Phys. Lett.* **1996**, *250*, 437.

(37) Tiede, D. M.; Choquet, Y.; Breton, J. *Biophys. J.* **1985**, *47*, 443.

(38) Parson, W. W.; Scherz, A.; Warshel, A. In *Antennas and Reaction Center of Photosynthetic Bacteria*; Michel-Beyerle, M. E., Ed; Springer-Verlag: Berlin Heidelberg, 1985; p 122.

(39) Hasegawa, J.; Nakatsuji, H. *J. Phys. Chem. B* **1998**, *102*, 10420.